JOC Article
pubs.acs.org/joc

Regioselectivity in the Nitration of Dialkoxybenzenes

Kevin Shopsowitz,[†] Francesco Lelj,*[,‡] and Mark J. MacLachlan*[,†]

[†]*Department of Chemistry, University of British Columbia, 2036 Main Mall, Vancouver, BC V6T 1Z1, Canada, and* [‡]*La.M.I. and LaSCAMM INSTM Sezione Basilicata, Dipartimento di Chimica, Università della Basilicata, Via dell'Ateneo Lucano 10, 85100 Potenza, Italy*

francesco.lelj@unibas.it; mmaclach@chem.ubc.ca

Received October 25, 2010

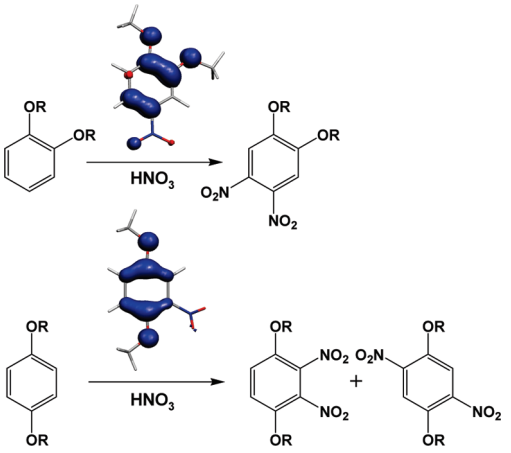

Dinitrodialkoxybenzene derivatives are important precursors for Schiff base macrocycles and a variety of other molecules. During our investigations, we have found that the dinitration reaction of 1,2-dialkoxybenzenes proceeds with unusual regioselectivity, giving exclusively the desired 1,2-dialkoxy-4,5-dinitrobenzene product, but we have been unable to find a good explanation for this result. The dinitration of 1,4-dialkoxybenzene derivatives also exhibits surprising regioselectivity that has hitherto been left unexplained. Herein, we report a detailed DFT analysis of the regioselective dinitration of both 1,2- and 1,4-dimethoxybenzene. These results show that the reaction mechanism likely involves a single electron transfer (SET) process. In the case of the former isomer, the regioselectivity is mainly determined by the symmetry of the HOMO of the aromatic moiety that defines the structure of the SHOMO of the aromatic radical cation formed by the SET process. In the case of the latter isomer, the selectivity is due mainly to solvation effects and may thus be altered depending on the solvent environment. Synthetic studies of the nitration of 1,4-dialkoxybenzene derivatives using different solvent conditions support this conclusion and provide practical information for tuning the regioselectivity of the reaction.

Introduction

Schiff base condensation is a convenient method for the construction of macrocycles[1,2] and complex structures.[3] We have been investigating macrocycles **4a**−**d**, which are prepared by the condensation of 1,2-dialkoxy-4,5-diaminobenzenes (e.g., **2a**−**d**) with dialdehyde **3**, Scheme 1.[4] These macrocycles with peripheral alkoxy chains exhibit interesting coordination and supramolecular chemistry.[5,6]

The preparation of macrocycles **4** requires diamines **2**, which are easily synthesized by the reduction of dinitroaryl compounds **1** (Scheme 1). In addition to their application in Schiff base macrocycle synthesis, 1,2-dialkoxy-4,5-dinitrobenzene compounds (e.g., **1a**−**d**) and their reduced diamine derivatives (e.g., **2a**−**d**) are useful precursors for many compounds, including liquid crystals,[7] optical materials,[8]

(1) (a) Borisova, N. E.; Reshetova, M. D.; Ustynyuk, Y. A. *Chem. Rev.* **2007**, *107*, 46–79. (b) Vigato, P. A.; Tamburini, S.; Bertolo, L. *Coord. Chem. Rev.* **2007**, *251*, 1311–1492. (c) MacLachlan, M. J. *Pure Appl. Chem.* **2006**, *78*, 873–888.

DOI: 10.1021/jo102113t Published on Web 01/31/2011

SCHEME 1. Synthesis of Macrocycles 4

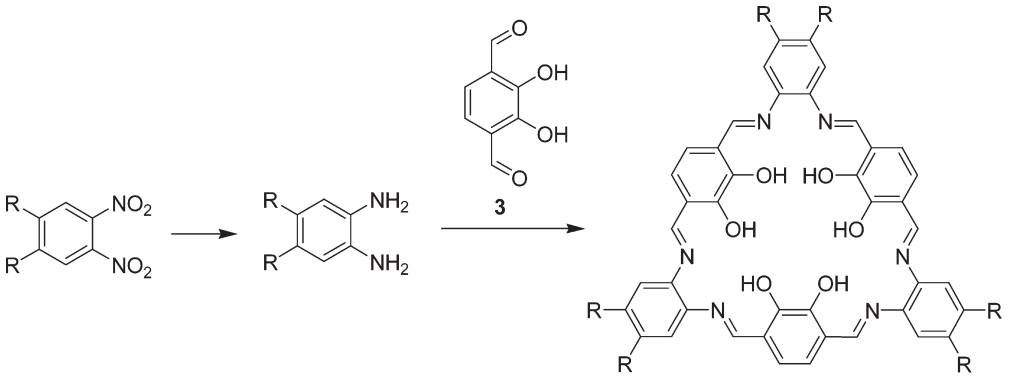

and pharmaceuticals.[9] Typically, the dinitroaryl compounds **1** are readily prepared by the nitration of 1,2-dialkoxybenzene derivatives in concentrated nitric acid, which almost exclusively yields the desired 4,5-dinitro product.[10] While this has been extremely beneficial to our study of Schiff base macrocycles, we have previously been unable to find an adequate explanation for this surprising regioselectivity.

Like their 1,2-dialkoxy counterparts, 1,4-dialkoxy-2,3-dinitrobenzene derivatives **5** are another class of compounds that are useful precursors for many different molecules, potentially including new Schiff base macrocycles. From the basic rules for electrophilic aromatic substitution, one would predict that the dinitration of 1,4-dimethoxybenzene (**8a**) would give primarily the 2,6-dinitro isomer **9** (favorable from the *o*,*p*-directing methoxy groups and the *m*-directing ability of the nitro group), with the 2,3-dinitro isomer being the least favored due to sterics; Scheme 3 shows the possible dinitration products. To our surprise, we found in the literature that nitration of 1,4-dimethoxybenzene yields only the 2,3-dinitro and 2,5-dinitro isomers **5a** and **10a**. Furthermore the relative amounts of **5a** and **10a** reported vary significantly from study to study depending on the conditions used.[11] Others have also expressed surprise at the regioselectivity of this reaction,[12] but we have been unable to find a good explanation for this result.

(2) For recent examples, see: (a) Akine, S.; Taniguchi, T.; Nabeshima, T. *Tetrahedron Lett*. **2001**, *42*, 8861–8864. (b) Gao, J.; Zingaro, R. A.; Reibenspies, J. H.; Martell, A. E. *Org. Lett*. **2004**, *6*, 2453–2455. (c) Gawronski, J.; Kwit, M.; Grajewski, J.; Gajewy, J.; Dlugokinska, A. *Tetrahedron: Asymmetry* **2007**, *18*, 2632–2637. (d) Korich, A. L.; Hughes, T. S. *Org. Lett*. **2008**, *10*, 5405–5408. (e) Kwit, M.; Zabicka, B.; Gawronski, J. *Dalton Trans*. **2009**, 6783–6789. (f) Frischmann, P. D.; Jiang, J.; Hui, J. K.-H.; Grzybowski, J. J.; MacLachlan, M. J. *Org. Lett*. **2008**, *10*, 1255–1258. (g) de Geest, D. J.; Noble, A.; Murray, K. S.; Larsena, D. S.; Brooker, S. *Dalton Trans*. **2007**, 467–475. (h) Hui, J. K.-H.; MacLachlan, M. J. *Chem. Commun*. **2006**, 2480–2482. (i) Givaja, G.; Volpe, M.; Edward, M. A.; Blake, A. J.; Wilson, C.; Schröder, M.; Love, J. B. *Angew. Chem., Int. Ed*. **2007**, *46*, 584–586. (j) Love, J. B. *Chem. Commun*. **2009**, 3154–3165. (k) Shimakoshi, H.; Takemoto, H.; Aritome, I.; Hisaeda, Y. *Tetrahedron Lett*. **2002**, *43*, 4809–4812.

(3) (a) Mastalerz, M. *Chem. Commun*. **2008**, 4756–4758. (b) Liu, X.; Liu, Y.; Li, G.; Warmuth, R. *Angew. Chem., Int. Ed*. **2006**, *45*, 901–904. (c) Içli, B.; Christinat, N.; Tönnemann, J.; Schüttler, C.; Scopelliti, R.; Severin, K. *J. Am. Chem. Soc*. **2009**, *131*, 3154–3155. (d) Sanmartín, J.; Bermejo, M. R.; García-Deibe, A. M.; Rivas, I. M.; Fernández, A. R. *J. Chem. Soc., Dalton Trans*. **2000**, 4174–4181. (e) Uribe-Romo, F. J.; Hunt, J. R.; Furukawa, H.; Klock, C.; O'Keeffe, M.; Yaghi, O. M. *J. Am. Chem. Soc*. **2009**, *131*, 4570–4571. (f) Tozawa, T.; et al. *Nat. Mater*. **2009**, *8*, 973–978. (g) Nitschke, J. R.; Schultz, D.; Bernardinelli, G.; Gérard, D. *J. Am. Chem. Soc*. **2004**, *126*, 16583–16543. (h) Nitschke, J. R.; Lehn, J.-M. *Proc. Natl. Acad. Sci. U. S. A*. **2003**, *100*, 11970–11974. (i) Chichak, K. S.; Cantrill, S. J.; Pease, A. R.; Chiu, S.-H.; Cave, G. W. V.; Atwood, J. L.; Stoddart, J. F. *Science* **2004**, *304*, 1308–1312.

(4) Gallant, A. J.; Hui, J. K.-H.; Zahariev, F. E.; Wang, Y. A.; MacLachlan, M. J. *J. Org. Chem*. **2005**, *70*, 7936–7946.

(5) (a) Gallant, A. J.; Chong, J. H.; MacLachlan, M. J. *Inorg. Chem*. **2006**, *45*, 5248–5250. (b) Frischmann, P. D.; Gallant, A. J.; Chong, J. H.; MacLachlan, M. J. *Inorg. Chem*. **2008**, *47*, 101–112. (c) Frischmann, P. D.; MacLachlan, M. J. *Chem. Commun*. **2007**, 4480–4482. (d) Nabeshima, T.; Miyazaki, H.; Iwasaki, A.; Akine, S.; Saiki, T.; Ikeda, C.; Sato, S. *Chem. Lett*. **2006**, *35*, 1070–1071. (e) Frischmann, P. D.; Facey, G. A.; Ghi, P. Y.; Gallant, A. J.; Bryce, D. L.; Lelj, F.; MacLachlan, M. J. *J. Am. Chem. Soc*. **2010**, *132*, 3893–3908.

(6) (a) Gallant, A. J.; MacLachlan, M. J. *Angew. Chem., Int. Ed*. **2003**, *42*, 5307–5310. (b) Hui, J. K.-H.; Frischmann, P. D.; Tso, C.-H.; Michal, C. A.; MacLachlan, M. J. *Chem.—Eur. J*. **2010**, *16*, 2453–2460.

(7) (a) Voisin, E.; Foster, E. J.; Rakotomalala, M.; Williams, V. E. *Chem. Mater*. **2009**, *21*, 3251–3261. (b) Glebowska, A.; Kamienska-Trela, K.; Krowczynski, A.; Pociecha, D.; Szydlowska, J.; Szczytko, J.; Twardowski, A.; Wojcik, J.; Gorecka, E. *J. Mater. Chem*. **2008**, *18*, 3419–3421. (c) Grolik, J.; Sieron, L.; Eilmes, J. *Tetrahedron Lett*. **2006**, *47*, 8209–8213. (d) Szydlowska, J.; Krowczynski, A.; Bilewicz, R.; Pociecha, D.; Glaz, L. *J. Mater. Chem*. **2008**, *18*, 1108–1115. (e) Durmus, M.; Dincer, F.; Ahsen, V. *Dyes Pigm*. **2008**, *77*, 402–407. (f) Hu, J.; Zhang, D.; Jin, S.; Cheng, S. Z. D.; Harris, F. W. *Chem. Mater*. **2004**, *16*, 4912–4915. (g) Sessler, J. L.; Callaway, W. B.; Dudek, S. P.; Date, R. W.; Bruce, D. W. *Inorg. Chem*. **2004**, *43*, 6650–6653. (h) Ong, C. W.; Liao, S.-C.; Chang, T. H.; Hsu, H.-F. *J. Org. Chem*. **2004**, *69*, 3181–3185. (i) Forget, S.; Veber, M.; Strzelecka, H. *Mol. Cryst. Liq. Cryst. Sci. Technol., Sect. A: Mol. Cryst. Liq. Cryst*. **1995**, *258*, 263–267.

(8) (a) Helgesen, M.; Gevorgyan, S. A.; Krebs, F. C.; Janssen, R. A. J. *Chem. Mater*. **2009**, *21*, 4669–4675. (b) Bouffard, J.; Swager, T. M. *Macromolecules* **2008**, *41*, 5559–5562. (c) Gautrot, J. E.; Hodge, P. *Polymer* **2007**, *48*, 7065–7077. (d) Wang, P.; Zhu, P.; Wu, W.; Kang, H.; Ye, C. *Phys. Chem. Chem. Phys*. **1999**, *1*, 3519–3525.

(9) (a) Pettit, G. R.; Thornhill, A. J.; Moser, B. R.; Hogan, F. *J. Nat. Prod*. **2008**, *71*, 1561–1563. (b) He, W.; Myers, M. R.; Hanney, B.; Spada, A. P.; Bilder, G.; Galzcinski, H.; Amin, D.; Needle, S.; Page, K.; Jayyosi, Z.; Perrone, M. H. *Bioorg. Med. Chem. Lett*. **2003**, *13*, 3097–3100. (c) Armer, R. E.; Barlow, J. S.; Dutton, C. J.; Greenway, D. H. J.; Greenwood, S. D. W.; Lad, N.; Tommasini, I. *Bioorg. Med. Chem. Lett*. **1997**, *7*, 2585–2588.

(10) (a) Leung, A. C. W.; MacLachlan, M. J. *J. Mater. Chem*. **2007**, *23*, 1923–1932. (b) Nose, M.; Suzuki, H. *Synthesis* **2000**, 1539–1542. (c) Ehrlich, J.; Bogert, M. T. *J. Org. Chem*. **1947**, *12*, 522–534. (d) Drake, N. L.; Anspon, H. D.; Draper, J. D.; Haywood, S. T.; Van Hook, J.; Melamed, S.; Peck, R. M.; Sterling, J., Jr.; Walton, E. W.; Whiton, A. *J. Am. Chem. Soc*. **1946**, *68*, 1536–1543. (e) Baker, M. V.; Brown, D. H.; Heath, C. H.; Skelton, B. W.; White, A. H.; Williams, C. C. *J. Org. Chem*. **2008**, *73*, 9340–9352. (f) Antonisse, M. M. G.; Snellink-Rueel, B. H. M.; Yigit, I.; Engbersen, J. F. J.; Reinhoudt, D. N. *J. Org. Chem*. **1997**, *62*, 9034–9038.

(11) (a) Besset, T.; Morin, C. *Synthesis* **2009**, 1753–1756. (b) Taleb, A.; Alvarez, F.; Nebois, P.; Walschofer, N. *Heterocycl. Commun*. **2006**, *12*, 111–114. (c) Fisher, G. H.; Moreno, H. R.; Oatis, J. E., Jr.; Schultz, H. P. *J. Med. Chem*. **1975**, *18*, 746–752. (d) Nose, M.; Suzuki, H. *Synthesis* **2000**, 1539–1542. (e) Mascal, M.; Yin, L.; Edwards, R.; Jarosh, M. *J. Org. Chem*. **2008**, *73*, 6148–6151.

(12) Dwyer, C. L.; Holzapfel, C. W. *Tetrahedron* **1998**, *54*, 7843–7848.

SCHEME 2. Proposed Synthesis of Macrocycles 7

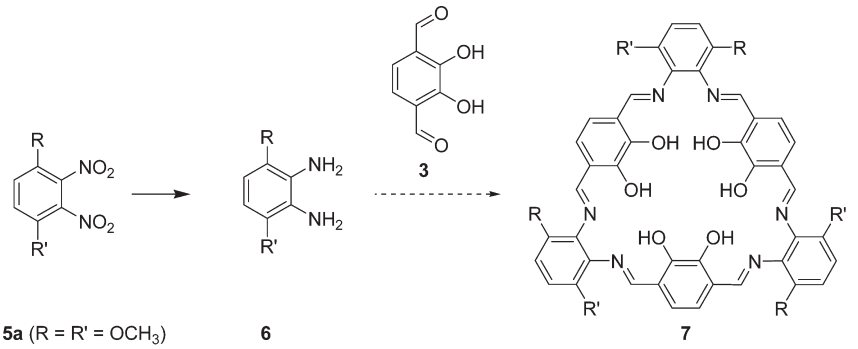

SCHEME 3. Possible Nitration Products from the Nitration of 8a

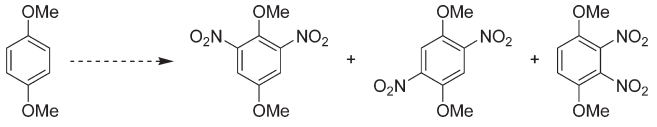

In this paper, we provide a detailed computational explanation for the regioselective dinitration of both 1,2- and 1,4-dimethoxybenzene. We also discuss the synthesis of some new 1,4-dialkoxydinitrobenzene derivatives and provide experimental observations on the effects of alkoxy chain length and solvent on the selectivity of the reaction.

Results and Discussion

The dinitration of 1,2-dialkoxybenzenes yields the 4,5-dinitro isomer as the only product regardless of which alkoxy chains are present. In contrast, the nitration of 1,4-dimethoxybenzene in concentrated nitric acid yields the 2,3-dinitro isomer as the major product and the 2,5-dinitro isomer as a minor product (~9:1). The introduction of different alkoxy chains and/or solvent conditions results in a change in the relative amounts of the 2,3- and 2,5-dinitro isomers formed from the reaction (Scheme 4, Table 7). In the following sections we provide a detailed computational and theoretical explanation for these unexpected regioselectivies and experimental observations that examine factors influencing the selectivity of the nitration of 1,4-dialkoxybenzenes.

Computational Studies of the Nitration of 1,2-Dialkoxybenzenes. Electrophilic aromatic substitution reactions have been thoroughly and intensively studied and debated for many years. Among these, nitration reactions have been assumed to proceed according to the same mechanism as other electrophilic reagents. In particular, it was thought that in the early stage of the reaction it proceeds according to the same mechanism as the class of reactions giving rise to a high-energy intermediate, the so-called Wheland adduct.[13] Besides the polar electrophilic reaction mechanism, a one-electron pathway was also proposed.[14,15] After 1977, this hypothesis was based on more solid grounds,[16] though some doubts were cast on this pathway in the case of aromatic compounds with lower ionization potentials.[17] According to this mechanism, it was suggested that the early stages of the nitration reaction could be related to an electron transfer process between the aromatic molecule and the NO_2^+ cation. Figure 1 shows the two different mechanisms.

The two-electron process assumes that the main process is related to the formation of an intermediate nitrated cationic species. In the single electron transfer (SET) model, the nitration reaction is a two-step redox process in which the NO_2^+ ion is first reduced by the aromatic molecule. The intimate complex of the two radicals then evolves into a cationic transition state that further yields the Wheland intermediate cationic species, which, after exchanging a proton by either an intra- or intermolecular (solvent) process, yields the nitroaromatic derivative.

The two possible mechanisms have been investigated by several computational approaches. Some early investigations, based on a single-determinant approach, mainly attempted to describe the transition states and intermediates for the Wheland mechanism,[18] while other authors have investigated the one-electron process in a multideterminantal framework.[19]

More recent computational investigations[20] have been undertaken at the DFT level and have discussed the first step in the nitration process. Upon changing the substituent on a monosubstituted benzene ring, the reaction can transform from a one-electron to a two-electron process.[21] An accurate multideterminantal investigation[22] compared the NO^+ and NO_2^+ electrophilic processes and concluded that in

(13) (a) Wheland, G. W. *J. Am. Chem. Soc.* **1942**, *64*, 900–908. (b) Wheland, G. W. *The Theory of Resonance*; Wiley: New York, 1944. (c) Olah, G. A. *Acc. Chem. Res.* **1971**, *4*, 240–248.

(14) Kenner, J. *Nature* **1945**, *156*, 369–370.

(15) Weiss, J. *Trans. Faraday Soc.* **1946**, *42*, 116–121.

(16) Perrin, C. L. *J. Am. Chem. Soc.* **1977**, *99*, 5516–5518.

(17) (a) Eberson, L.; Jönsson, L.; Radner, F. *Acta Chem. Scand. B* **1978**, *32*, 749–753. (b) Eberson, L.; Radner, F. *Acta Chem. Scand. B* **1980**, *34*, 739. (c) Eberson, L.; Radner, F. *Acc. Chem. Res.* **1987**, *20*, 53–59.

(18) Chen, L.; Xiao, H.; Xiao, J.; Gong, X. *J. Phys. Chem. A* **2003**, *107*, 11440–11444.

(19) (a) Peluso, A.; Del Re, G. *J. Phys. Chem.* **1996**, *100*, 5303–5309. (b) Albunia, A. R.; Borrelli, R.; Peluso, A. *Theor. Chem. Acc.* **2000**, *104*, 218–222.

(20) Esteves, P. M.; Carneiro, J. W. D.; Cardoso, S. P.; Barbosa, A. G. H.; Laali, K. K.; Rasul, G.; Prakash, G. K. S.; Olah, G. A. *J. Am. Chem. Soc.* **2003**, *125*, 4836–4849.

(21) de Queiroz, J. F.; Carneiro, J. W. D..; Sabino, A. A.; Sparrapan, R.; Eberlin, M. N.; Esteves, P. M. *J. Org. Chem.* **2006**, *71*, 6192–6203.

(22) (a) Gwaltney, S. R.; Rosokha, S. V.; Head-Gordon, M.; Kochi, J. K. *J. Am. Chem. Soc.* **2003**, *125*, 3273–3283. (b) Rosokha, S. V.; Kochi, J. K. Charge-Transfer Effects on Arene Structure and Reactivity. In *Modern Arene Chemistry*; Astruc, D., Ed.; Wiley-VCH Verlag GmbH & Co. KGaA: Weinheim, 2002; pp 435−478.

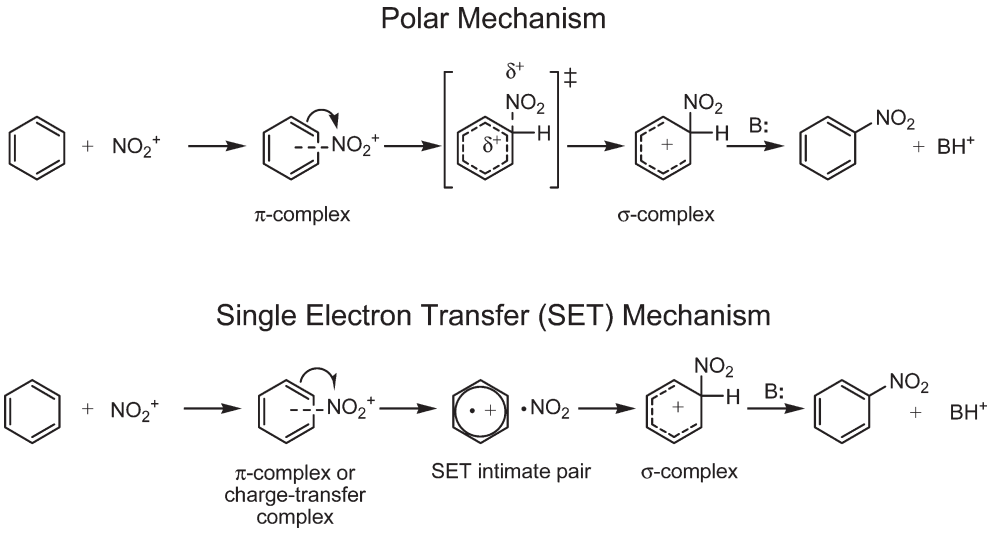

FIGURE 1. Two possible mechanisms proposed for the nitration of benzene. Adapted from ref 21.

SCHEME 4. Nitration of 1,4-Dialkoxybenzene Derivatives 8a−d

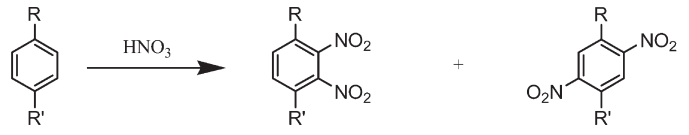

8a (R = R' = OMe)
8b (R = R' = OBu-n)
8c (R = R' = OHex-n)
8d (R = OMe, R' = OHex-n)

5a (R = R' = OMe)
5b (R = R' = OBu-n)
5c (R = R' = OHex-n)
5d (R = OMe, R' = OHex-n)

10a (R = R' = OMe)
10b (R = R' = OBu-n)
10c (R = R' = OHex-n)
10d (R = OMe, R' = OHex-n)

the case of the benzene molecule they can both be described as single electron transfer processes. According to this view, the NO_2^+ cation is first π-coordinated to the benzene molecule (the precursor complex, PC). Further electron transfer generates the $^{\cdot}NO_2$ radical π-coordinated to the rim of the benzene radical cation at a distance of 2.175 Å. In the case of benzene as the substrate, the rate-determining step appears to be the transformation of the PC to the σ complex (successor complex, SC). The last step is the scission of the C−H bond in the σ complex, which is fast and, in the case of the benzene molecule, shows no deuterium isotope effect. This process can be intra- or intermolecular if an opportune Lewis base accepts the proton from the protonated aromatic molecule. A further process involves the 1,2 migration of the NO_2 moiety between adjacent carbon atoms. For the benzene molecule, this has a very low activation barrier comparable to the PC−SC energy barrier.[20]

The potential energy surface for the interaction of NO_2^+ and benzene is very complex, and many intermediates and side products have been documented.[20] On the other hand no previous studies have been performed on multisubstituted benzene rings. Last, but not least, the contribution of solvation effects cannot be underestimated due to the different polarization induced by and on the solvent in the case of different isomers. It has been shown that this can be very relevant in the case of nitration processes on benzene molecules.[18]

For purposes of computation, we examined the mechanism of nitration of 1,2-dimethoxy-4-nitrobenzene (1,2-DMNB), which is the intermediate in the double nitration of veratrole. For 1,2-DMNB, the interaction energy surface with a NO_2^+ ion has been computed as a function of two spherical angular variables, as defined in Figure 2. The aromatic moiety has been assumed rigid, and the NO_2^+ ion's geometrical parameters, the separation between the center of the aromatic ring and the nitrogen atom, and the NO_2^+ moiety's orientation relative to the aromatic molecule have been fully optimized. Starting from the geometry of the most stable structures, whose angular (θ, ϕ) parameters are close to the 3, 4, and 5 unsubstituted positions, the molecular energy has been further minimized in the space of the whole set of molecular geometric parameters.

A plot of the energy as a function of the θ,ϕ angular parameters is shown in Figure 3. Energies corresponding to the same ϕ angle are connected. Superimposed on this plot is the aromatic molecule. It can easily be seen that the most stable adduct is the one on the rim of the aromatic ring close to the C2 position (see blue and indigo lines). This adduct is characterized by a zenith angle in the range of 20−30°, hence close to the perpendicular of the aromatic molecule, suggesting that the most stable adduct should be the ipso one on the C2 π system. In fact, in the case of a monosubstituted benzene ring, the possibility of an ipso adduct has also been reported[23] along with the formation of adducts on the carbons bearing hydrogen atoms.[24] This has been discussed

(23) Perrin, C. L.; Skinner, G. A. *J. Am. Chem. Soc.* **1971**, *93*, 3389–3394.
(24) De Queiroz, J. F.; Carneiro, J. W. D.; Sabino, A. A.; Sparrapan, R.; Eberlin, M. N.; Esteves, P. M. *J. Org. Chem.* **2006**, *71*, 6192–6203.

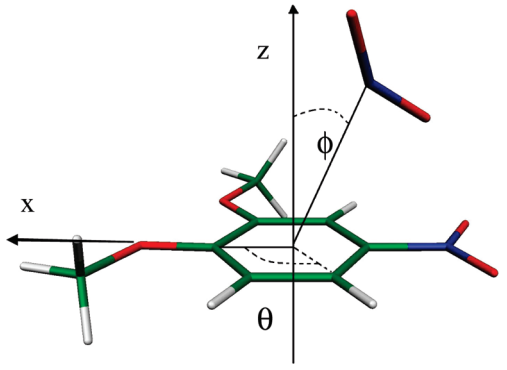

FIGURE 2. Angular parameters ϕ (zenith) and θ (azimuth) are defined as used in the potential energy map.

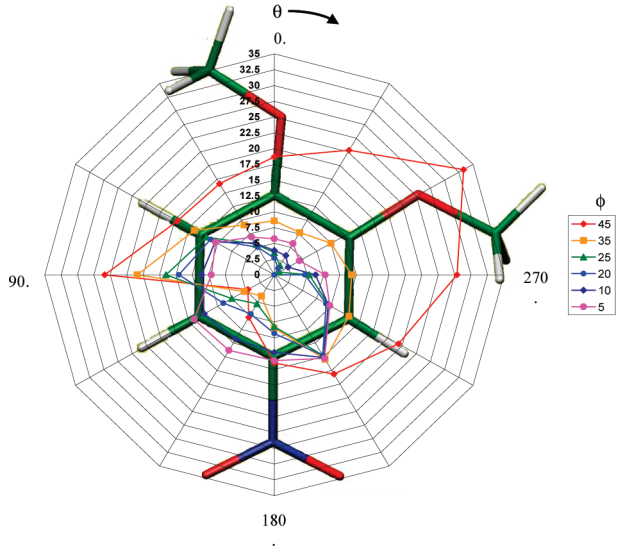

FIGURE 3. Energy as a function of angular parameters for the approach of NO_2^+ to 1,2-dimethoxy-4-nitrobenzene (1,2-DMNB). In each colored trace, the energy (kcal/mol) is radially plotted for the same ϕ-value (5−45°) as a function of the in-plane angle θ (0−360°). Thus, points corresponding to lower energy are closer to the center. For each point, the distance of the nitrogen atom of the NO_2 moiety from the center of the aromatic ring was optimized for minimum energy, but this distance is not represented on the graph.

and taken into account in order to explain in general the ipso substitution products[23,25] that are obtained in the case of good leaving groups such as *tert*-butyl and trimethylsilyl on the benzene ring[26] (different products are formed in the reaction due to the nature of the group present in the ipso position; see ref [23]) and to explain the composition of the ions found in MS studies.[24]

A value for ϕ around 45° shows low energy values in the plot region around θ = 120°. This is reminiscent of a geometry akin to the Wheland intermediate. It is worth noting that this position is the only one in which the energy decreases when going from ϕ = 5° to 45°. Positions C3 and C6 show an increase in energy going from 5° to 45°, the former showing the largest gradient.

The energies of the different Wheland intermediates have been computed with full geometry optimization starting from the most stable structures that were previously located. From Table 1 it can be seen that the adduct stability order is C5 ≈ C1−C2 (π) ≫ C6 ≈ C3. Indeed the last structure can be obtained only by an NO_2^+ migration from the π adduct on the rim between the C1 and C2 carbon atoms with a transition state (C1−C2)→C3. In fact the lowest energy structure obtained from the previous map always ended with a π adduct on the molecular rim between C1 and C2. This pattern suggests that substitution in position 5 should be the most easily reached, and it could be directly obtained in the case of an approach from the top of the molecule (ϕ close to the vertical to the molecular plane and θ values in the range 140−160°). We have performed different searches starting from several starting positions of the NO_2^+ cation on top of 1,2-DMNB. It appears that two different products are always obtained. The C2 adduct is obtained if the starting position of the NO_2^+ cation is far from the benzene ring (4.5 Å) irrespective of whether it is closer to the C3 or C5 atoms. Conversely, the process always ends on the C5 atom if the NO_2^+ is closer (3.5 Å) to the 1,2-DMNB molecule and at the same distance from C3 and C5. This reaction pathway is followed without any activation energy and proceeds smoothly with the bending of the NO_2^+ from 180° to the final angle of ∼134°. Other substitutions require larger modifications of the electronic structure and proceed through multiple steps around the rim of the aromatic molecule. This pathway has already been pointed out in the case of the benzene molecule.

The (C1−C2)→C3 pathway has been further checked by computing the intrinsic reaction coordinate (IRC)[27] in both directions along the transition vector corresponding to the negative Hessian eigenvalue starting from the found transition state.

The study of the different pathways suggests that the NO_2 moiety can move around the ring starting from the π-bonded adduct near C2 or C4 toward different carbon atoms generating the Wheland adducts. These processes go through transition states, whose energies are reported in Table 2.

Figure 4 reports the trend of the electrostatic potential evaluated at a van der Waals distance from each atom in the case of the neutral molecule. The trend of the electrostatic potential is well synthesized by the net atomic charges computed according to the Merz−Kollman approach (Table 3).[28]

As a general observation, all methods for computing charge distribution both in the neutral molecule and in the corresponding radical cation (Tables 3 and 4) are unable to pinpoint the complexity and the essential physics of the interaction process between NO_2^+ and the aromatic molecule. To some extent only NBO charges suggest that the interaction of the NO_2^+ ion should prefer the interaction with C5 rather than C3 but fail completely to predict the good π interaction with C2. On the other hand, spin density (see Figure 5) suggests that among the substituted carbon atoms C2 should be the most reactive, whereas C5 should be

(25) (a) Olah, G. A.; Malhotra, R.; Narang, S. C. *Nitration Methods and Mechanism*; VCH: New York, 1989. (b) Nightingale, D. V. *Chem. Rev.* **1947**, *40*, 117–140. (c) Moodie, R. B.; Schofield, K. *Acc. Chem. Res.* **1976**, *9*, 287–292. (d) Attina, M.; Cacace, F.; Ricci, A. *J. Phys. Chem.* **1996**, *100*, 4424–4429.

(26) Eaborn, C. *Organosilicon Compounds*; Academic Press: New York, 1960.

(27) (a) Gonzalez, C.; Schlegel, H. B. *J. Chem. Phys.* **1989**, *90*, 2154–2161. (b) Gonzalez, C.; Schlegel, H. B. *J. Phys. Chem.* **1990**, *94*, 5523–5527.

(28) Besler, B. H.; Merz, K. M., Jr.; Kollman, P. A. *J. Comput. Chem.* **1990**, *11*, 431–439.

TABLE 1. Energies and Relevant Parameters for the NO_2^+ Adducts of 1,2-DMNB

adduct	molecular energy[a] (hartree)	relative energy (kcal/mol)	ZPE (hartree)	molecular energy[a] + ZPE (hartree)	relative energy (kcal/mol)
π C1−C2	−870.286 777	0.9	0.179 442	−870.107 335	0.0
σ C3	−870.281 342	4.4	0.180 684	−870.100 656	4.2
π C4	−870.282 138	3.9	0.180 013	−870.102 125	3.3
σ C5	−870.288 289	0.0	0.180 586	−870.107 220	0.1
σ C6	−870.280 377	5.0	0.180 577	−870.099 820	4.7

[a]Nuclear + electronic contributions.

TABLE 2. Transition-State Energies and Imaginary Frequencies of 1,2-DMNB

TS	molecular energy[a] (hartree)	imaginary frequency (cm^{-1})	ZPE (hartree)	molecular energy[a] + ZPEc (hartree)	relative energy (kcal/mol)
(C1−C2)→C6	−870.273 998	147	0.179 174	−870.094 824	4.5
(C1−C2)→ C3	−870.278 265	118	0.179 585	−870.098 680	1.8
C4→ C3	−870.262 062	391	0.178 110	−870.083 952	12.0
C4→ C5	−870.281 176	72	0.179 418	−870.101 758	0.0

[a]Nuclear + electronic contributions.

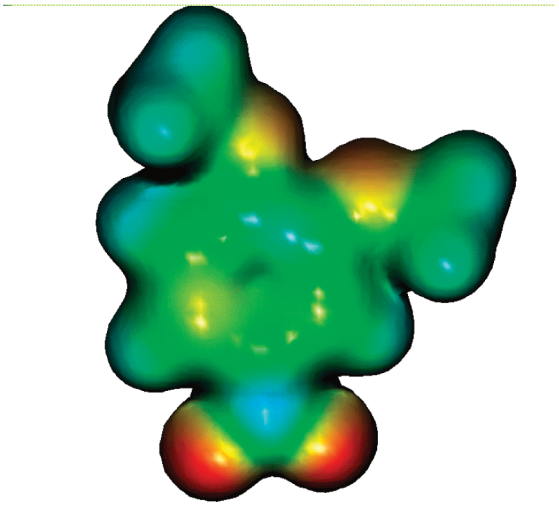

FIGURE 4. Electrostatic potential computed at van der Waals distance (red: negatively charged; blue: positively charged).

TABLE 3. 1,2-DMNB Net Atomic Charges According to Different Approaches for the Neutral Molecule (atomic units)

atom	Mulliken	NBO[29,a]	ESP[b]
C1	−0.339	+0.326	+0.265
C2	−0.095	+0.296	+0.294
C3	+0.489	−0.301	−0.213
C4	−1.071	+0.051	+0.044
C5	−0.044	−0.215	−0.289
C6	+0.642	−0.217	−0.186

[a]NBO: natural bond orbital. [b]ESP: electrostatic potential.

TABLE 4. 1,2-DMNB Radical Cation Net Atomic Charges and Spin Densities on the Aromatic Carbon Atoms (atomic units)

atom	Mulliken	NBO[a]	ESP[b]	spin
C1	+0.124	+0.358	−0.304	+0.210
C2	+0.105	+0.392	−0.010	+0.225
C3	−0.138	−0.289	+0.236	−0.030
C4	−0.005	+0.106	−0.915	+0.157
C5	−0.136	−0.141	+0.205	+0.131
C6	−0.134	−0.216	+0.613	−0.052

[a]NBO: natural bond orbital. [b]ESP: electrostatic potential.

the one where the most stable Wheland adduct should be formed after reduction of the NO_2^+ and oxidation of the aromatic molecule. This behavior strongly hints that in this case the nitration process should be related to a SET process and that dimethoxy

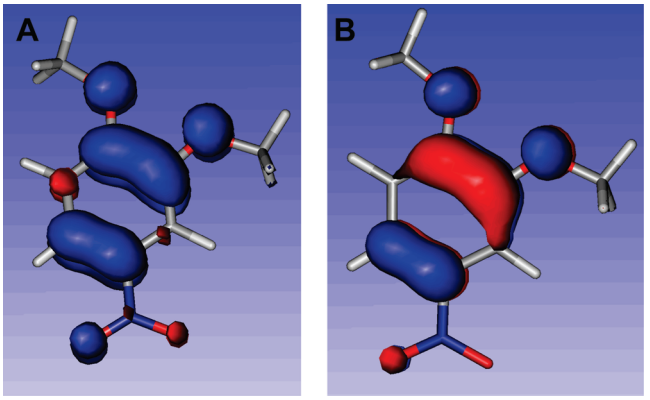

FIGURE 5. (A) 1,2-DMNB cation spin density (blue = spin density increase; red = spin density depletion). (B) 1,2-DMNB cation SHOMO (red and blue refer to the sign of the wave function).

substitution turns the 1,2-DMNB into a good reducing agent toward NO_2^+ irrespective of the presence of the nitro group.

This is confirmed by the comparison of the relaxed ionization potential of 1,2-DMNB and the electron affinity of NO_2^+, computed using the energies of the cation and the neutral molecules at the same level of approximation, which are 8.03 and −8.32 eV (experimental = −9.586 ± 0.002 eV),[21] respectively. These results lead to an exothermic reaction energy of 0.29 eV or 6.69 kcal/mol (1.55 eV or 31.8 kcal/mol if using the experimental value). With this large reaction energy the SET intermediate cannot be trapped and the process directly affords the Wheland σ adduct.[16]

The high selectivity for position 5 is easily understood by looking at the plot of the spin density.[16] From Figure 5 it is evident that the molecule is split into two different basins: one related to the two OMe groups and the other containing the C4 and C5 atoms. Carbons C3 and C6 have reduced spin densities due to the nodal structure of the SHOMO, which shows a nodal plane perpendicular to the average molecular plane and passing through C3−C6 atoms. The origin of the SHOMO can be easily understood by taking into account the interaction between the two OMe groups and the benzene doubly degenerate highest occupied orbital. The NO_2 fragment orbitals are very low in energy due to the large electronegativity of all constituent atoms and give a negligible contribution to the resulting MOs, even if it is enough to remove the equivalence of the C1 and C2 atoms as far as the spin density is concerned.

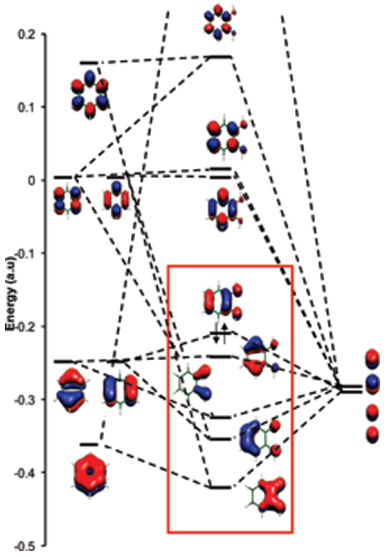

FIGURE 6. Schematic orbital interaction diagram between the benzene MOs (left) and the symmetry-adapted π orbitals of the two OMe fragments (right). The occupied orbitals are shown in the red box. The two arrows depict the electrons in the HOMO.

The two OMe oxygen atoms give rise to an almost degenerate set of bonding−antibonding orbitals. Indeed the small distance between the two oxygen atoms and the resulting nonzero overlap between the π orbitals removes the degeneracy between the couple.

Owing to the symmetry of benzene's MO characterized by the nodal plane perpendicular to the average molecular plane and passing through the C3−C6 atoms, the interaction with the bonding combination of the two OMe fragment orbitals generates a bonding and an antibonding orbital (Figure 6). The resulting orbitals are both occupied, and the one reported in Figure 5B is the HOMO. This MO gives rise to the spin density reported in Figure 5A when one electron is removed.

Computational Studies of the Nitration of 1,4-Dialkoxybenzenes. In the case of 1,4-OR substitution, the distance between the two oxygen atoms is very large and the couple is degenerate. In this case, the interaction is with the other e_{1g} benzene orbital and the resulting MOs (bonding and antibonding combination) preserve the nodal plane perpendicular to the C2−C3 and C5−C6 bonds. In this way the incipient NO_2 radical does not have any definite preferred interaction site with developing spin density on the incipient aromatic radical cation (if not for the small perturbation due to inductive effects through the σ skeleton).

Table 5 reports the results for the complexes in the case of 1,4-DMNB. As with 1,2-DMNB, the most stable π-adducts are the ipso ones, in this case on C1 and C4, whose stability order is C1 > C4, in agreement with the spin densities of the radical cation of 1,4-DMNB. As for the σ adducts at positions 3, 5, and 6, in spite of the fact that the spin densities on these carbon atoms are in the order C5 > C6 > C3, the interaction energy under vacuum indicates that the adduct stability order is C5 > C3 > C6 and the C5 adduct is the most stable isomer. On the other hand it can be seen that after we introduce the solvation contribution of water to the molecular energy the trend is modified and the relative stability order of the adducts becomes C3 > C5 > C6. The difference in energy of 2.48 millihartree corresponds to 1.50 kcal mol^{-1}, which at 27 °C gives a K_{eq} that corresponds to a C3:C5 substitution ratio of ~10:1.

Besides the direct addition to the carbon atoms that gives rise directly to the substitution products, we also investigated the possibility of NO_2 moiety migration between adjacent carbon atoms. In this case the transition-state energy for the migration C4→C5 is also lower than that for C4→C3 in the gas phase, and the introduction of a solvation contribution results in the C4→C3 transition-state energy becoming lower (see Table 6). These data suggest that the C5 adduct could be the most stable in nonpolar solvents or in the gas phase, whereas the C3 adduct is favored in polar environments such as concentrated nitric acid. Furthermore, in polar environments, the C3 isomer is the most abundant product both in the case of a direct addition to the hydrogen-bearing carbon atom or when the first adduct is on the carbon atom bearing the more electron-donating alkoxy group. Because the NO_2^+ ion adds from "above" the aromatic ring and the linear aliphatic substituents are always far apart from the reactive centers, an increase in the bulkiness of substituents on the C1 and C4 atoms should not be able to reverse the relative abundance of the C3/C5 products. However, more specific solvent distribution around the aromatic molecule modulated by the different bulkiness or hydrophobicity of the aliphatic substituent can modify the relative contribution of the solvation energy and modify to some extent the actual ratio of the two isomers formed. Moreover, in the case of very bulky substituents whose structure can influence the ipso position (e.g., O^{t}Bu), the stability of the π ipso adduct can be affected, and this can potentially influence the C3/C5 adducts ratio.

Synthetic Studies of the Nitration of 1,4-Dialkoxybenzenes Supporting Computational Studies. We undertook a series of experiments to support the computational results for the nitration of 1,4-dialkoxybenzenes (Scheme 4). From the calculations, in nonpolar environments the 2,5-dinitro isomer should be favored, whereas in strongly polar solvent environments the opposite is expected. Indeed, we found that the nitration of dialkoxy benzenes **8a**−**d** in concentrated nitric acid all result in the 2,3-dinitro isomer being formed as the major product. However, the ratio of 2,3-dinitro isomer relative to 2,5-dinitro isomer obtained from the nitration of **8b**−**d** is considerably less compared to that obtained from the nitration of **8a** (Table 7). Although it seemed plausible that the increased steric bulk in **8b**−**d** may have been responsible for the shift in selectivity, our computational studies suggested that steric effects should be insignificant and that solvation is the dominant factor influencing selectivity. To further test this, we isolated the mixed-alkoxy-mononitro compounds **11a** and **11b** and subjected them to a second nitration reaction (Scheme 5). If steric effects were significant, we would expect different selectivities for the two mononitro compounds. Instead we found that the same ratio of dinitration products is obtained from the nitration of **11a** and **11b**, indicating that steric effects do not play a major role.

In previous studies, the nitration of 1,4-dimethoxybenzene (**8a**) has been carried out using different solvent systems and has led to variable proportions of 2,3-dinitro:2,5-dinitro

(29) Carpenter, J. E.; Weinhold, F. *J. Mol. Struct.* (*THEOCHEM*) **1988**, *169*, 41–62.

TABLE 5. Spin Densities of Radical Cation, Energies (hartree), and Relative Energies for Different Adducts of 1,4-DMNB

atom/isomer	spin density (radical cation)	molecular energy (ΔE) $[DMNB\text{-}NO_2]^+$	ZPE	ΔE + ZPE	rel. energy (kcal/mol)	ΔE_{sol} + ZPE	rel. energy (kcal/mol)
C1 (π)	0.223	−870.282 466	0.179 655	−870.102 811	0.00	−870.187 517	2.53
C2	0.019						
C3	0.038	−870.278 850	0.180 241	−870.098 609	2.64	−870.191 542	0.00
C4 (π)	0.221	−870.282 082	0.179 636	−870.102 446	0.23	−870.189 133	1.51
C5	0.082	−870.280 345	0.180 162	−870.100 183	1.65	−870.189 141	1.50
C6	0.059	−870.268 875	0.180 176	−870.088 700	8.85		

TABLE 6. $[1,4\text{-DMNB-}NO_2]^+$ Transition-State Energies (hartree) for the Indicated Processes

TS	molecular energy	ZPE	ΔE_{sol}	ΔE_{sol} + ZPE	$\Delta E^{\ddagger}_{sol}$ + ZPE	imaginary frequency (cm^{-1})
C4→C3	−870.278 146	0.17948	−870.366 198	−870.186 72	3.03	54.6
C4→C5	−870.278 754	0.17920	−870.363 305	−870.184 10	4.67	62.7

TABLE 7. Relative Amount of Regioisomers Formed from the Nitration of 8a−d in Concentrated Nitric Acid[a]

precursor	alkoxy chains	% 2,3-isomer	% 2,5-isomer
8a	R = R′ = OMe	88	12
8b	R = R′ = OBu-n	60	40
8c	R = R′ = OHex-n	59	41
8d	R = OMe, R′ = OHex-n	66	34

[a] [**8a−d**] = 0.72 M.

isomers depending on the conditions that were employed.[11] We decided to use acetic anhydride combined with concentrated nitric acid as a system to study the influence of solvent polarity on the selectivity of the dinitration reaction. Overall we studied the nitration of **8a** using four different conditions ranging in solvent polarity with the most polar condition being concentrated nitric acid (Figure 7). Two nitration conditions of intermediate solvent polarity were examined by mixing acetic anhydride and concentrated nitric acid in different ratios prior to the addition of **8a**. For the least polar nitration condition, **8a** was first dissolved in acetic anhydride and concentrated nitric acid was then slowly added to the solution. In agreement with the theoretical prediction, a clear increase in the formation of the 2,5-dinitro isomer is observed with decreasing solvent polarity. In the case of the least polar nitration condition, the 2,5-dinitro isomer is favored over the 2,3-dinitro isomer by a 2:1 ratio, which to the best of our knowledge is the highest regioselectivity for 1,4-dimethoxy-2,5-dinitrobenzene that has been reported. This is compared to an 8:1 ratio favoring the 2,3-dinitro isomer when the nitration is performed in concentrated nitric acid. Mixed dialkoxyaryl compound **8d** was also nitrated using this latter condition (**8b** and **8c** could not be studied due to poor solubility in acetic anhydride at 0 °C); in contrast to the results for concentrated nitric acid, the ratios of 2,3-dinitro and 2,5-dinitro isomers for the nitrations of **8a** and **8d** are virtually identical. We believe that this is further evidence that the solvent environment determines the regioselectivity considering that both **8a** and **8d** were completely dissolved prior to the addition of nitric acid. These results lead us to postulate that the different selectivities observed for the double nitration of **8b−d** compared with 1,4-dimethoxybenzene (**8a**) in concentrated nitric acid are simply due to shielding from the polar solvent environment by the hydrophobic alkoxy chains.

To further understand the mechanism of the dinitration, we undertook ^{15}N-labeling experiments. The ^{15}N-labeled

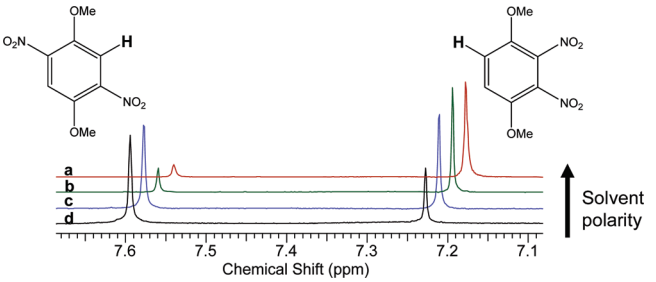

FIGURE 7. ^1H NMR spectra ($CDCl_3$) of the aromatic regions for the nitration of **8a** using different solvent conditions: (a) concentrated nitric acid; (b) AcOAc/HNO_3 (0.54:1 v/v); (c) AcOAc/HNO_3 (0.14:1 v/v); (d) AcOAc followed by the slow addition of HNO_3. Spectra are offset and the residual solvent peaks (7.27 ppm) were removed for clarity.

SCHEME 5. Nitration of Mononitrodialkoxybenzenes 11a and 11b

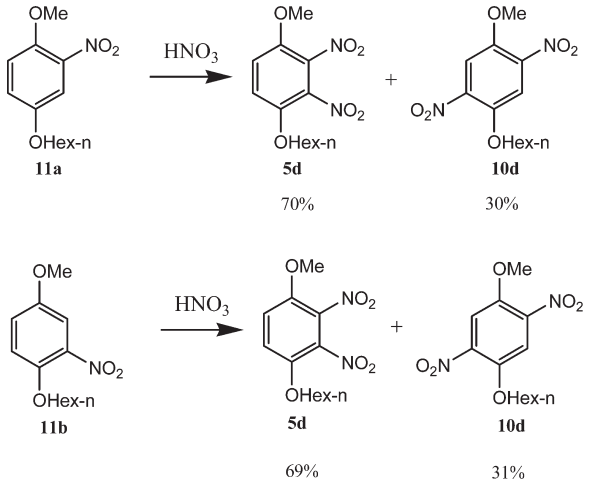

version of **11b** (^{15}N-**11b**) was synthesized by mononitrating **8d** using $K^{15}NO_3$. ^{15}N-**11b** was subjected to concentrated nitric acid at 80 °C, conditions that readily lead to the doubly nitrated products shown in Scheme 6. After 1 h at 80 °C the crude product was isolated and consisted of the 2,3-dinitro and 2,5-dinitro isomers. EI-MS revealed the presence of $^{15}N/^{14}N$ dinitro products, while only trace amounts of $^{14}N/^{14}N$ products were detected. This indicates that the second nitration step is essentially irreversible, and therefore no intermolecular scrambling occurs.

SCHEME 6. Products Obtained from the Nitration of ^{15}N-11b in Concentrated Nitric Acid (80 °C, 1 h)

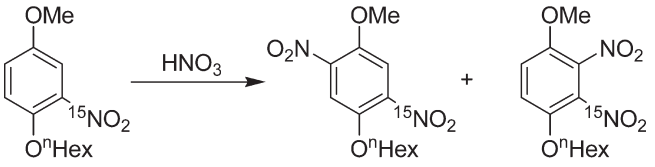

^{15}N-**11b**

Conclusions

Detailed calculations were carried out to better understand the unexpected selectivity observed for the dinitration of 1,2-dialkoxy- and 1,4-dialkoxybenzenes. In the case of the nitration of 1,2-dialkoxybenzenes, the exclusive formation of the 4,5-dinitro-substituted product can be explained on the basis of the single electron transfer mechanism and simple molecular orbital arguments. For the dinitration of 1,4-dialkoxybenzenes, DFT calculations indicated that the 2,3-dinitro and 2,5-dinitro products should both be formed and that the relative amounts should mostly be influenced by the solvent environment as opposed to steric and inductive electronic influences. Nitration experiments carried out on a variety of 1,4-dialkoxybenzene derivatives support these conclusions, confirming that the steric environment of the benzene ring in 1,4-dialkoxybenzenes appears to have no influence on selectivity, whereas the choice of solvent system has a large effect. Finally we show that this information may be used to rationally tune the regioselectivity of the reaction.

Experimental Section

Calculations. Gaussian03 (revision D.02)[30] has been used for all the computations. Density functional theory (DFT) has been applied by using the Schmider and Becke hybrid xc functionals[31] and 6-31++G(d,p)[32] basis set. All of the stationary structures found have been verified to be minima by computing the Hessian matrix. All energies are corrected by the zero point energy (ZPE) contribution. Solvation effects have been taken into account by the IEPCM[33] without further geometry optimization. Molecular structures have been drawn with the programs GaussView3.0 and Molekel4.3.[34] All computations have been mainly performed using model compounds 1,2-dimethoxy-4-nitrobenzene (1,2-DMNB) and 1,4-dimethoxy-2-nitrobenzene (1,4-DMNB).

Synthesis. Compounds **8b**,[35] **8c**,[36] and **8d**[37] were prepared by literature methods. The ratios of 2,3-dinitro:2,5-dinitro regioisomers were calculated by integrating the peaks assigned to the aromatic C−H groups in the ^{1}H NMR spectra. All reactions were carried out under air unless otherwise noted.

Procedure for the Nitration of 8 in Concentrated Nitric Acid (8a as an example). 1,4-Dimethoxybenzene (1.0 g, 7.2 mmol) was slowly added to 10 mL of concentrated nitric acid chilled on an ice/water bath. The reaction mixture was stirred at 0 °C for 1 h, then stirred at room temperature for 1 h, and finally heated to 80 °C for 1 h. The dark orange reaction mixture was then poured into ∼30 mL of ice water, resulting in the formation of a yellow precipitate. This was then filtered and washed with a large amount of water, giving the crude product (1.4 g, 85%) as a mixture of 2,3- and 2,5-dinitro-1,4-dimethoxybenzene (**5a** and **10a**, respectively). ^{1}H NMR spectroscopy was conducted on the crude isolated product in order to determine the relative amounts of **5a** and **10a** formed.

General Procedure for the Isolation of 5b−d and 10b−d (5b and 10b as examples). The crude product (2.5 g) from the nitration of 1,4-dibutyloxybenzene (**8b**) was separated by column chromatography (silica gel, petroleum ether/ethyl acetate = 4:1). 1,4-Dibutyloxy-2,5-dinitrobenzene (**10b**, 0.79 g, 2.5 mmol, 32%) was isolated as the faster moving band. After all of the 2,5-dinitro isomer had been collected (as monitored by TLC), the second fraction was eluted with toluene, giving 1,4-dibutyloxy-2,3-dinitrobenzene (**5b**, 1.0 g, 3.2 mmol, 40%).

1,4-Dibutyloxy-2,3-dinitrobenzene (5b). ^{1}H NMR ($CDCl_3$, 400 MHz): δ 0.96 (t, J = 7.5 Hz, 6H), 1.42−1.52 (h, J = 7.5 Hz, 4H), 1.73−1.80 (p, J = 7.5 Hz, 4H), 4.07 (t, J = 7.5 Hz, 4H), 7.16 (s, 2H). ^{13}C{^{1}H} NMR ($CDCl_3$, 100 MHz): δ 13.6, 18.9, 30.9, 70.8, 117.8, 134.7, 144.8. MS (EI): m/z 312 (M^+). IR ν (neat): 2956, 2873, 1536, 1490, 1351, 1274, 1153, 1051, 1029, 936, 807, 755, 623, 538 cm^{-1}. Mp = 66−68 °C. Anal. Calcd for $C_{14}H_{20}N_2O_6$: C, 53.84, H, 6.45, N, 8.97. Found: C, 53.90, H, 6.53, N, 9.04.

1,4-Dihexyloxy-2,3-dinitrobenzene (5c). ^{1}H NMR ($CDCl_3$, 400 MHz): δ 0.91 (t, J = 7.0 Hz, 6H), 1.30−1.36 (m, 8H), 1.43 (p, J = 7.2 Hz, 4H), 1.78 (p, 7.2 Hz, 4H), 4.06 (t, 6.5 Hz, 4H), 7.16 (s, 2H). ^{13}C{^{1}H} NMR ($CDCl_3$, 100 MHz): δ 13.9, 22.5, 25.3, 28.8, 31.4, 71.1, 117.8, 134.7, 144.8. MS (EI): m/z 368 (M^+). IR ν (neat): 2952, 2929, 2870, 1545, 1496, 1465, 1359, 1272, 1156, 1042, 802, 725, 626, 544 cm^{-1}. Mp = 48−50 °C. Anal. Calcd for $C_{18}H_{28}N_2O_6$: C, 58.68, H, 7.66, N, 7.60. Found: C, 58.81, H, 7.42, N, 7.75.

1-Hexyloxy-4-methoxy-2,3-dinitrobenzene (5d). ^{1}H NMR ($CDCl_3$, 400 MHz): δ 0.90 (t, J = 7.0 Hz, 3H), 1.31−1.36 (m, 4H), 1.43 (p, J = 7.0 Hz, 2H), 1.77 (p, J = 7.5 Hz, 2H), 3.93 (s, 3H), 4.07 (t, J = 6.5 Hz, 2H), 7.19 (s, 2H). ^{13}C{^{1}H} NMR ($CDCl_3$, 100 MHz): δ 14.2, 22.8, 25.7, 29.1, 31.6, 57.9, 71.4, 117.0, 118.2, 134.7, 135.0, 145.3, 145.5. IR ν (neat): 2932, 2844, 1533, 1491, 1441, 1349, 1273, 1154, 1061, 1015, 924, 789, 733, 606 cm^{-1}. Mp = 82−84 °C. HRMS: calcd for $C_{13}H_{18}N_2O_6$ $[M]^+$ 298.11649, found 298.11664.

1,4-Dibutyloxy-2,5-dinitrobenzene (10b). ^{1}H NMR ($CDCl_3$, 300 MHz): δ 0.98 (t, J = 7.5 Hz, 6H), 1.46−1.58 (h, J = 7.5 Hz, 4H), 1.78−1.87 (p, J = 7.5 Hz, 4H), 4.11 (t, J = 7.5 Hz, 4H), 7.52 (s, 2H). ^{13}C{^{1}H} NMR ($CDCl_3$, 100 MHz): δ 13.7, 19.0, 30.8, 70.6, 111.9, 142.0, 145.5. MS (EI): m/z 312 (M^+). IR ν (neat): 2959, 2933, 2873, 1536, 1462, 1391, 1344, 1276, 1220, 1064, 985, 877, 789, 757, 628, 539 cm^{-1}. Mp = 132−135 °C. Anal. Calcd for $C_{14}H_{20}N_2O_6$: C, 53.84, H, 6.45, N, 8.97. Found: C, 53.39, H, 6.38, N, 9.19.

1,4-Dihexyloxy-2,5-dinitrobenzene (10c). ^{1}H NMR ($CDCl_3$, 400 MHz): δ 0.92 (t, J = 6.7 Hz, 6H), 1.32−1.37 (m, 8H), 1.48 (p, J = 7.5 Hz, 4H), 1.83 (p, J = 7.5 Hz, 4H), 4.10 (t, J = 6.5 Hz, 4H), 7.51 (s, 2H). ^{13}C{^{1}H} NMR ($CDCl_3$, 100 MHz): δ 13.9, 22.5, 25.4, 28.7, 31.3, 70.9, 111.9, 142.0, 145.5. MS (EI): m/z 368

(30) Frisch, M. J.; et al. *Gaussian 03*, Revision D.02; Gaussian, Inc.: Wallingford, CT, 2004.
(31) Schmider, H. L.; Becke, A. D. *J. Chem. Phys.* **1998**, *108*, 9624–9631.
(32) (a) Ditchfield, R.; Hehre, W. J.; Pople, J. A. *J. Chem. Phys.* **1971**, *54*, 724–728. (b) Hehre, W. J.; Ditchfield, R.; Pople, J. A. *J. Chem. Phys.* **1972**, *56*, 2257–2261. (c) Rassolov, V. A.; Pople, J. A.; Ratner, M. A.; Windus, T. L. *J. Chem. Phys.* **1998**, *109*, 1223–1229. (d) Clark, T.; Chandrasekhar, J.; Spitznagel, G. W.; Schleyer, P. v. R. *J. Comput. Chem.* **1983**, *4*, 294–301.
(33) (a) Cammi, R.; Mennucci, B.; Tomasi, J. *J. Phys. Chem. A* **2000**, *104*, 5631–5637. (b) Cammi, R.; Mennucci, B.; Tomasi, J. *J. Phys. Chem. A* **1999**, *103*, 9100–9108. (c) Mennucci, B.; Cancès, E.; Tomasi, J. *J. Phys. Chem. B* **1997**, *101*, 10506–10517. (d) Cossi, M.; Scalmani, G.; Rega, N.; Barone, V. *J. Chem. Phys.* **2002**, *117*, 43–54.
(34) Flükiger, P.; et al. *MOLEKEL 4.3*; Swiss Center for Scientific Computing: Manno, Switzerland, 2002.
(35) Liu, X.; Zhou, X.; Shu, X.; Zhu, J. *Macromolecules* **2009**, *42*, 7634–7637.
(36) Ramesh, A. R.; Thomas, K. G. *Chem. Commun.* **2010**, *46*, 3457–3459.
(37) Altman, R. A.; Shafir, A.; Choi, A.; Lichtor, P. A.; Buchwald, S. L. *J. Org. Chem.* **2008**, *73*, 284–286.

(M^+). IR ν (neat): 2957, 2930, 2859, 1534, 1392, 1270, 1224, 996, 877, 794, 759 cm^{-1}. Mp = 111−113 °C. Anal. Calcd for $C_{18}H_{28}N_2O_6$: C, 58.68, H, 7.66, N, 7.60. Found: C, 58.68, H, 7.59, N, 7.75.

1-Hexyloxy-4-methoxy-2,5-dinitrobenzene (10d). ^{1}H NMR ($CDCl_3$, 300 MHz): δ 0.91 (t, J = 7.0 Hz, 3H), 1.32−1.37 (m, 4H), 1.48 (p, J = 7.0 Hz, 2H), 1.84 (p, J = 7.5 Hz, 2H), 3.98 (s, 3H), 4.11 (t, J = 6.4 Hz, 2H), 7.54 (s, 2H). $^{13}C\{^1H\}$ NMR ($CDCl_3$, 100 MHz): δ 14.2, 22.8, 25.7, 29.0, 31.6, 57.7, 71.2, 111.3, 112.4, 142.0, 142.3, 146.0, 146.2. MS (EI): m/z 298 (M^+). IR ν (neat): 2933, 2858, 1547, 1519, 1473, 1351, 1278, 1226, 1004, 882, 787, 593, 555 cm^{-1}. Mp = 93−96 °C. Anal. Calcd for $C_{13}H_{18}N_2O_6$: C, 52.34, H, 6.08, N, 9.39. Found: C, 52.31, H, 6.06, N, 9.52.

Preparation of 1-Hexyloxy-4-methoxy-3-nitrobenzene (11a). 1-Hexyloxy-4-methoxybenzene (0.50 g, 2.4 mmol) was added to a solution of 1.5 mL of concentrated nitric acid dissolved in 10 mL of ethyl acetate at room temperature. After stirring the reaction mixture at room temperature for 18 h, 40 mL of ethyl acetate and 50 mL of water were added. The organic phase was isolated, then washed with 2 × 30 mL of water, dried over $MgSO_4$, and filtered. Removal of the solvent under vacuum gave a dark orange oil (340 mg, 1.34 mmol, 56%) consisting of the two mononitro isomers. Column chromatography (silica gel, hexanes/ethyl acetate = 9:1) was used to isolate **12a** as the slower moving fraction (orange oil, 100 mg, 0.39 mmol, 17%).

1-Hexyloxy-4-methoxy-3-nitrobenzene (11a). ^{1}H NMR ($CDCl_3$, 400 MHz): δ 0.92 (t, J = 7.5 Hz, 3H), 1.32−1.38 (m, 4H), 1.44−1.48 (m, 2H), 1.78 (p, J = 7.5 Hz, 2H), 3.92 (s, 3H), 3.95 (t, J = 7.5 Hz, 2H), 7.02 (d, J = 10 Hz, 1H), 7.09−7.12 (m, 1H), 7.39 (d, J = 4.5 Hz, 1H). $^{13}C\{^1H\}$ NMR ($CDCl_3$, 100 MHz): δ 14.0, 22.5, 25.6, 29.1, 31.5, 57.1, 69.1, 110.7, 115.1, 121.4, 139.6, 147.2, 152.5. IR ν (neat): 2930, 2858, 1526, 1466, 1350, 1272, 1218, 1019, 812, 771, 743, 547 cm^{-1}. HRMS: calcd for $C_{13}H_{19}NO_4$ $[M]^+$ 253.13141, found 253.13130.

Preparation of 1-Hexyloxy-4-methoxy-2-nitrobenzene (11b). Potassium carbonate (1.64 g, 21.8 mmol), 1-bromohexane (1.66 mL, 11.8 mmol), and sodium iodide (100 mg, 0.67 mmol) were added to a solution of 4-methoxy-2-nitrophenol (2.0 g, 11.8 mmol) dissolved in 40 mL of acetone. The reaction mixture was then heated to reflux for 16 h. The cloudy red reaction mixture was filtered, and then the solvent was removed under vacuum. Water (100 mL) was added to the oily red residue, and the product was then extracted with 3 × 50 mL of dichloromethane. The combined organic fractions were washed with 2 × 50 mL of 5% NaOH solution and 50 mL of water, dried over $MgSO_4$, and then filtered. An orange oil was obtained after the solvent was removed under vacuum. The oil was filtered through a short silica plug with 20:1 petroleum ether/ethyl acetate, resulting in a pale yellow solution. The solvent was removed under vacuum, yielding **12b** as a yellow oil (1.73 g, 6.8 mmol, 57%).

1-Hexyloxy-4-methoxy-2-nitrobenzene (11b). ^{1}H NMR ($CDCl_3$, 300 MHz): δ 0.91 (t, J = 7.5 Hz, 3H), 1.31−1.38 (m, 4H), 1.45−1.53 (m, 2H), 1.82 (p, J = 7.5 Hz, 2H), 3.82 (s, 3H), 4.05 (t, J = 7.5 Hz, 2H), 7.02 (d, J = 10 Hz, 1H), 7.07−7.11 (m, 1H), 7.38 (d, J = 4.5 Hz, 1H). $^{13}C\{^1H\}$ ($CDCl_3$, 100 MHz): δ 13.9, 22.5, 25.5, 29.1, 31.4, 56.0, 70.5, 109.7, 116.4, 120.7, 140.0, 146.8, 152.8. MS (EI): m/z 253 (M^+). IR ν (neat): 2930, 2858, 1526, 1498, 1466, 1349, 1277, 1219, 1150, 1037, 913, 855, 808, 778, 747, 562 cm^{-1}. Anal. Calcd for $C_{13}H_{19}NO_4$: C, 61.64, H, 7.56, N, 5.53. Found: C, 61.74, H, 7.50, N, 5.68.

Preparation of ^{15}N-1-Hexyloxy-4-methoxy-2-nitrobenzene (^{15}N-11b). 1-Hexyloxy-4-methoxybenzene (**8d**, 0.50 g, 2.4 mmol) was slowly added to a solution of $K^{15}NO_3$ (0.26 g, 2.6 mmol) and *p*-toluenesulfonic acid (0.57 g, 3.0 mmol) in 7.5 mL of acetic anhydride chilled on an ice/water bath. Following the addition, the reaction mixture was allowed to stir at RT for 18 h. After the addition of 30 mL of water, the organic phase was extracted with 3 × 20 mL of DCM. The organic fractions were combined, washed with water (3 × 30 mL), and dried over $MgSO_4$. The solvent was removed under vacuum, leaving behind a dark yellow oil consisting of the two mononitro isomers. ^{15}N-**11b** was isolated by column chromatography (silica gel, hexanes/ethyl acetate = 9:1) as the faster moving fraction (160 mg, 0.63 mmol, 26%). The product was confirmed by ^{1}H NMR spectroscopy and EI-MS (m/z 254 (M^+)).

Nitration Study of 1,4-Dimethoxybenzene (8a) in Acetic Anhydride and Nitric Acid. Three different solvent conditions were used and are labeled according to the scheme given in the caption for Figure 7. **b:** 1,4-Dimethoxybenzene (**8a**, 0.50 g, 3.6 mmol) was slowly added to a mixture of 7.4 mL of acetic anhydride and 4 mL of concentrated nitric acid chilled to 0 °C in an ice/water bath. This mixture was stirred on ice for 1 h, then at room temperature for 1 h, and finally heated to 80 °C for 1 h. The reaction mixture was poured into ∼30 mL of ice/water, resulting in the formation of a yellow precipitate. This was then isolated on a Buchner funnel, rinsed with water, and then air-dried to give a mixture of 2,3- and 2,5-dinitro-1,4-dimethoxybenzene (715 mg, 3.1 mmol, 87%). ^{1}H NMR spectroscopy was used to determine the ratio of 2,3-dinitro and 2,5-dinitro isomers formed. **c:** The same procedure was employed except that the volumes of acetic anhydride and concentrated nitric acid used were 10 and 1.4 mL, respectively. **d:** Compound **8a** was dissolved in 10 mL of acetic anhydride and chilled in an ice/water bath. Then 1.4 mL of concentrated nitric acid was added dropwise with vigorous stirring. The reaction mixture was allowed to stir on ice for 1 h, then at RT for 1 h, and finally for 1 h at 80 °C. The reaction mixture was poured into ∼30 mL of ice/water, resulting in the formation of a yellow precipitate, which was isolated by vacuum filtration, rinsed with water, and air-dried to give a mixture of 2,3- and 2,5-dinitro-1,4-dimethoxybenzene (740 mg, 3.2 mmol, 90%). Procedure **d** was also used for the nitration of **8d**.

Acknowledgment. We thank UBC and NSERC (Discovery Grant) for funding. K.E.S. thanks NSERC for a postgraduate fellowship. F.L. is grateful to INSTM and the Project "Call for Ideas" of Università della Basilicata for the year 2010 for financial support.

Supporting Information Available: Text and figures giving details of computation coordinates and characterization data (^{1}H NMR, ^{13}C NMR, MS). This material is available free of charge via the Internet at http://pubs.acs.org.